

Chapter 2

The Solar Energy Resource

The sun shone, having no alternative, on the nothing new

Samuel Beckett, Routledge, London (1938)

2.1 Overview

The earth rotates at an axial tilt in an elliptical orbit around the sun producing the annual variation of intensity outside the earth's atmosphere (Lunde 1980) shown in Fig. 2.1. Beneath the atmosphere solar energy varies temporally and geographically in its

- Intensity
- The relative magnitudes of its direct and diffuse components and
- The skyward anisotropy of the diffuse component and
- In its spectral compositions.

Ninety nine percent of the thickness of the earth's atmosphere lies within a distance of about 30 km from the earth's surface. In passing through the atmosphere solar radiation is reflected, absorbed and scattered, diminishing total insolation and reducing its direct beam component. The intensity of solar energy received by a surface at ground level depends on the orientation of the surface in relation to the sun, the hour of day, the day of the year, the latitude and altitude at the point of observation and atmospheric conditions. The key factors that determine how much solar energy leaving the Sun is incident on a specific surface plane on earth are summarised in Fig. 2.2. Incident radiation from the sun arrives at the earth with a $1/2^\circ$ cone. When passing through a turbid atmosphere with large aerosol content of this angular cone broadens due to forward scattering. This broader cone is referred to as circumsolar radiation. In a clear atmosphere, direct solar radiation forms a large proportion of the solar radiation incident at the earth's surface. In a cloudy atmosphere, diffuse radiation becomes a significant fraction of the total solar radiation as a result of the scattering of the direct beam by clouds.

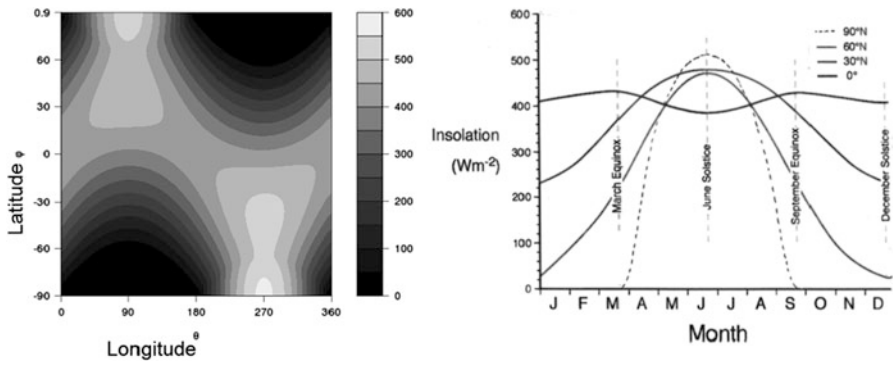


Fig. 2.1 Insolation on a horizontal plane just above the earth's atmosphere

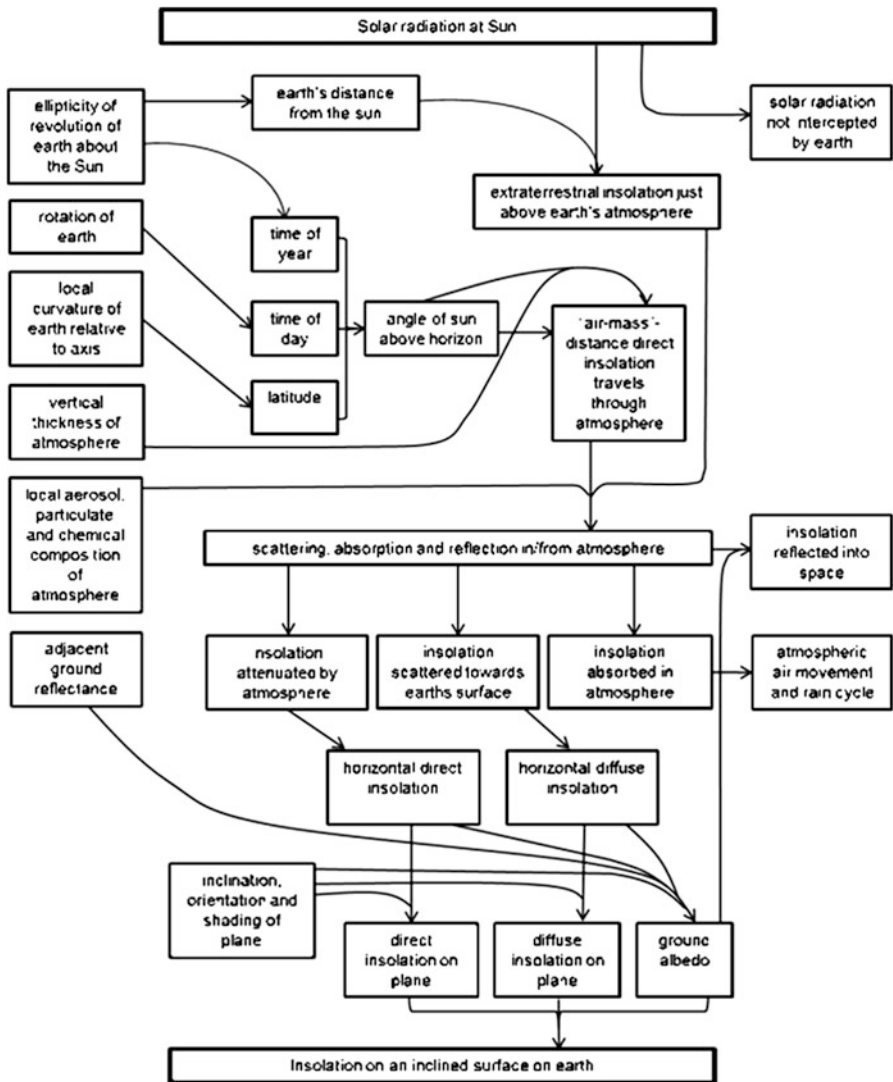


Fig. 2.2 Solar energy interception between emission from sun to a surface plane on earth

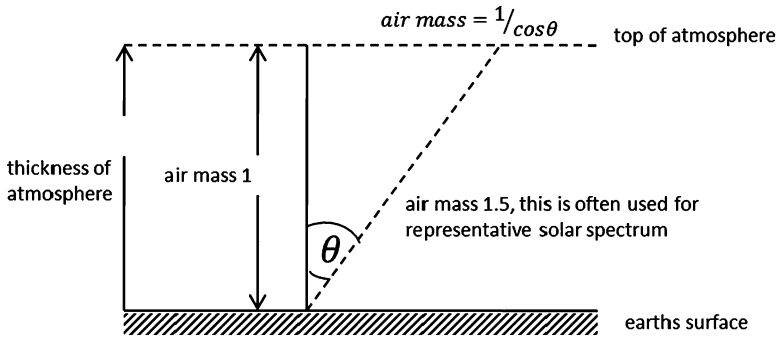


Fig. 2.3 Definition of air-mass

Scattered solar energy incident on the ground forms the diffuse insolation component. The extent of absorption and scattering of radiation by the atmosphere depends on the air-mass, i.e. length of the path traversed and the composition of the atmosphere. The traversed path for beam radiation is shortest when the sun is at zenith, the beam follows an inclined path in reaching the earth's surface. Air mass is defined as shown in Fig. 2.3.

Solar energy is radiation in a specific range the electromagnetic spectrum shown in Fig. 2.4. In passing through the atmosphere, ozone, water vapour dioxide, nitrogen, oxygen, aerosols, dust particles, and clouds all selectively attenuate particular solar radiation wavelengths by either absorption or scattering. Ozone, concentrated in a layer between 10 and 30 km above the earth's surface, with maximum concentration occurring between about 25 and 30 km, is a very strong absorber of solar radiation in the ultraviolet range between 0.2 and 0.29 μm , a relatively strong absorber in the range 0.29–0.34 μm and has a weak absorption in the range 0.44–0.7 μm . There are both geographic and seasonal variations in ozone concentration. Water vapour absorbs solar radiation strongly in wavelengths beyond about 2.3 μm with several absorption bands in the range of wavelengths between 0.7 and 2.3 μm . Oxygen absorbs solar radiation in a region of 0.762 μm . Carbon dioxide is a strong absorber of solar radiation in wavelengths beyond 2.2 μm . The effect of such absorptions on the solar spectrum received at the surface of the earth is summarised in Fig. 2.5.

Both the diurnal and annual patterns of insolation are stochastic in nature. In many climates it is not possible to predict exactly the insolation at any particular instant. However such instantaneous single values usually aggregate to form robust long-term statistical distributions. Thus it is possible to know that specific values for insolation *will* occur within a particular period of time but not precisely *when* within the period. Such correlations enable prediction of insolation in the absence of measured data. However they should be used with care as they cannot always be reliably extrapolated to different locations, even those with a similar climate (Van den Brink 1982).

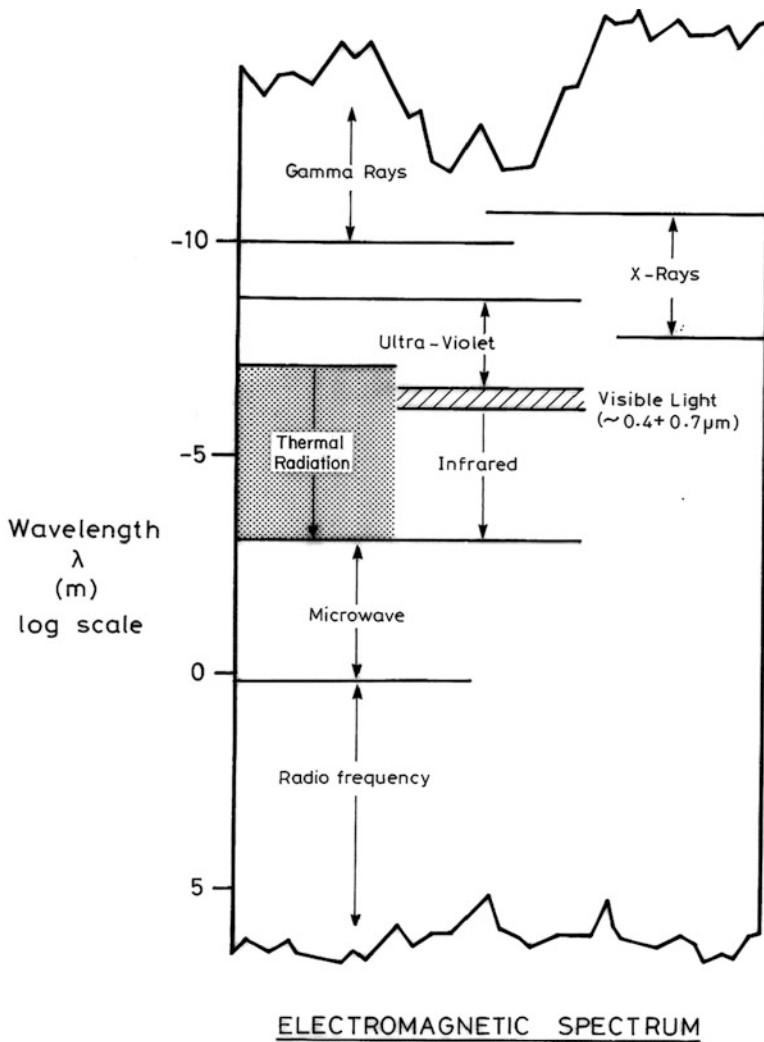


Fig. 2.4 Electromagnetic spectrum

2.2 Terrestrial Measurement of Solar Energy

Daily and hourly records of the amount of solar radiation received at any given location over the earth's surface have been essential for the design and optimisation of thermophysical systems utilising solar energy. Therefore, solar radiation measurements are made continuously at monitoring stations located at different parts of the world. Such measurements include the;

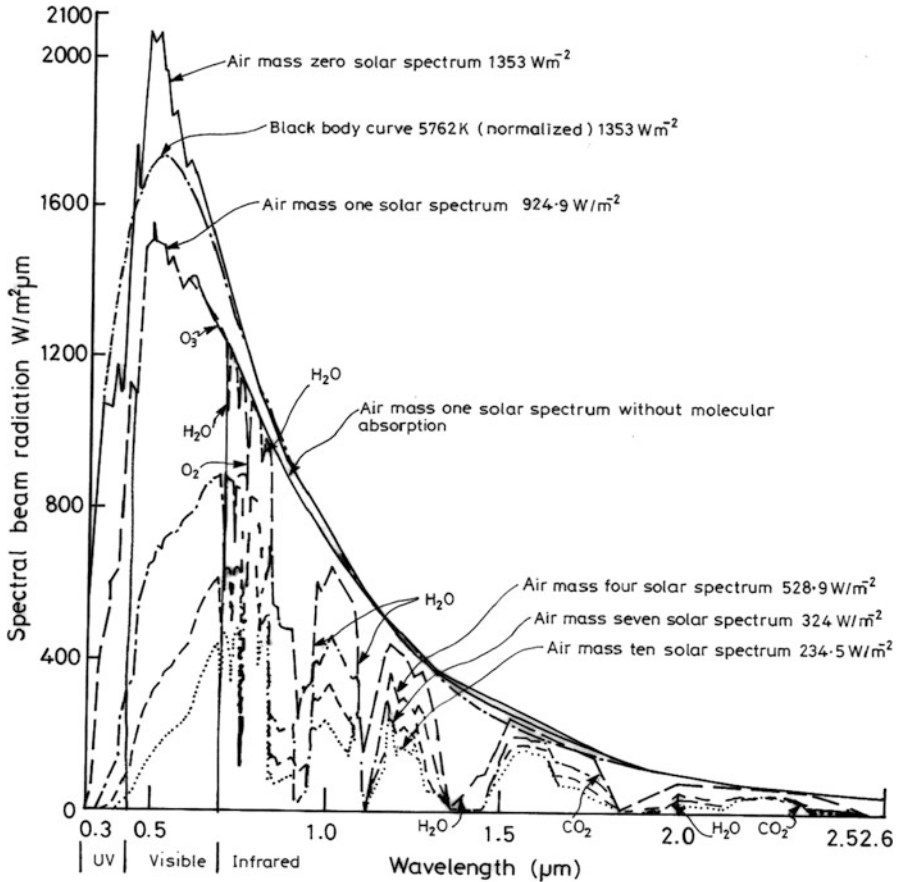
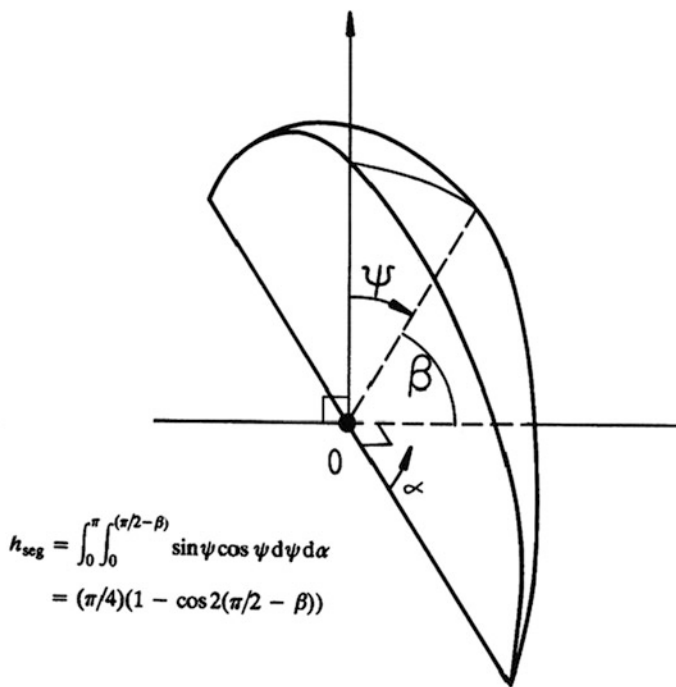


Fig. 2.5 Solar spectrum as attenuated by passage through different air masses

- Intensity of direct solar radiation at normal incidence
- Diffuse component on a horizontal surface
- Global solar radiation on a horizontal surface
- Total solar radiation on an inclined surface at a specified orientation
- Spectral distribution of over certain wavelength bands
- Solar radiation reflected from the ground

Instruments used for the measurement of solar radiation are either: pyranometers or pyrhemeliometers. A pyranometer measures the total solar radiation incident on a horizontal surface from the entire sky as shown in Fig. 2.6. A pyrhemeliometer measures the intensity of the direct solar radiation at normal incidence.

Diffuse solar radiation is measured most commonly by attaching a shadow-band to a pyranometer to obscure the direct rays of the sun from the sensing element. Commonly used constant-diameter shadow-bands are moved along an axis, parallel to the earth's axis, according to the solar declination angle. To determine shadow band



The total radiation sensed by a solarimeter, without a shadow-band, from a hemisphere, radius $a/\cos \delta$, is

$$H = (h_s + h_g)a^2/\cos^2 \delta$$

Fig. 2.6 Total radiation used by a solarimeter without a shadow band

correction factors on inclined planes under overcast conditions (Burek et al. 1988), a pair of pyranometers are mounted side-by-side on an adjustable-inclination south-facing plane; one measures global insolation, the other, fitted with a shadow band, measures diffuse. Both the shadow-band and the inclination of the solarimeters are adjusted periodically (e.g., every 2 weeks) to maintain the dome of the diffuse-measuring pyranometer in shadow and ensure that insolation is measured normal to the sun's rays at solar noon respectively. During uniformly cloudy conditions when the insolation is solely diffuse and isotropic, if no correction were necessary for the shadow-band then the measurements from the global-radiation pyranometer and the diffuse-radiation pyranometer with a shadow-band would be identical. In reality, the ratio of the measured total insolation to the measured diffuse insolation under such sky conditions is the correction factor required when using a shadow-band. This factor enables inclusion of the diffuse radiation from the direction of the sun obscured by the shadow band. The error is small, and for most applications, there is no need to distinguish between diffuse and direct radiation from the same direction. Because the shadow band need only be adjusted to correct for variations in the sun's declination angle only once every 7–14 days, simple methods (Burek et al. 1988) have practical

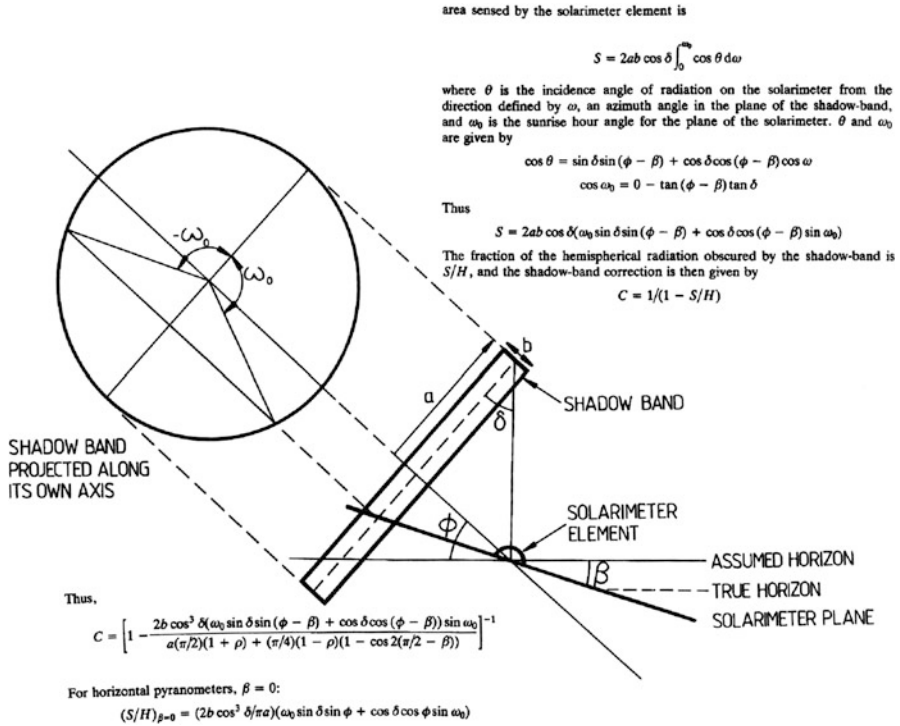


Fig. 2.7 Shadow band correction factors for inclined and a horizontal solarimeters

advantages when compared with the more accurate shade-disc method. The latter compares the ‘true’ value of diffuse radiation, as measured with a solarimeter fitted with a moving shade disc to obscure the direct radiation, with the reading from the pyranometer fitted with the shadow-band.

The geometry of the shadow-band in relation to the solarimeter has been analysed to determine the variation of the correction factor for horizontal solarimeters with the time of year, as a function of the solar declination and the sunrise and sunset hour angles (Drummond 1956; Robinson and Stoch 1964) and south-facing (in the northern hemisphere) inclined planes (Burek et al. 1988). Such a geometric correction as shown in Fig. 2.7 assumes implicitly an isotropic distribution of diffuse radiation. Anisotropic diffuse radiation introduces an error of only a few percent in an isotropic (i.e. geometric) correction (Ineichen et al. 1983). Only where such accuracy is essential should shadow-band corrections be used to account for anisotropic diffuse sky radiation. Either empirical or analytical distributions of diffuse radiation for clear skies can be used as neither approach is consistently better than the other (Rawlins and Readings 1986). Empirical correction methods have been based either on the time of year and the measured ratio of diffuse to global radiation (Painter 1981) or on global radiation, because the anisotropy of diffuse radiation can be related to this parameter (Mujahid and Turner 1980).

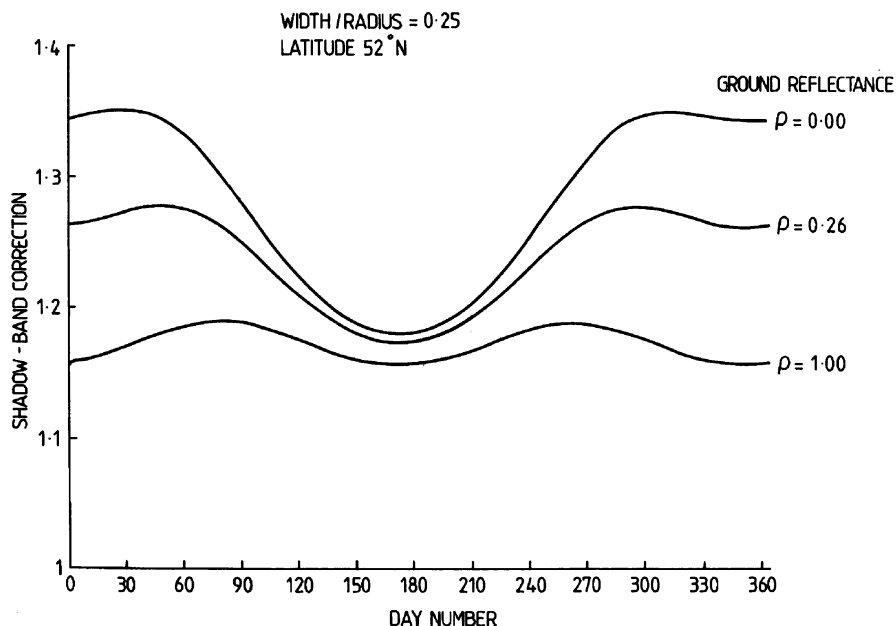


Fig. 2.8 Shadow band correction factors for a pyranometer perpendicular to solar incidence at solar noon

An analytical and experimental study of the effect of part of the inner surface of the shadow-band being illuminated by direct sunlight, especially at low solar altitudes showed that the effect of the width of the shadow-band on the anisotropy correction (considered separately from the geometric correction) was not significant (Steven and Unsworth 1980), except for very narrow bands, with width-to-radius ratio less than 0.15. It has been found that Drummond's (1956) correction function that implicitly assumed an isotropic radiation distribution was in reasonable agreement with daily-averaged data for cloudy days, whereas a correction with an anisotropic distribution fitted the data more closely for clearer days (Ineichen et al. 1983). Anisotropy correction of diffuse radiation measurements is thus, somewhat ironically, of some relevance for very accurate measurements of low diffuse insolation conditions.

The shadow band correction factors for inclined and horizontal solarimeter elements subject to a uniform solar radiation flux, are shown in Fig. 2.8 in which the incidence angle of radiation on the solarimeter is related to an azimuth angle in the plane of the shadow-band, and the sunrise hour angle for the plane of the solarimeter.

When seen from an altitude, the horizon of a flat landscape is below the horizontal; for example at an altitude of 5 m, the horizon is at an angle 2.2° below horizontal. For a roof-mounted pyranometer the shadow-board correction factors should include an altitude amendment to avoid an incorrectly high value. Additional correction is also required for inclined surfaces; Fig. 2.7 shows the

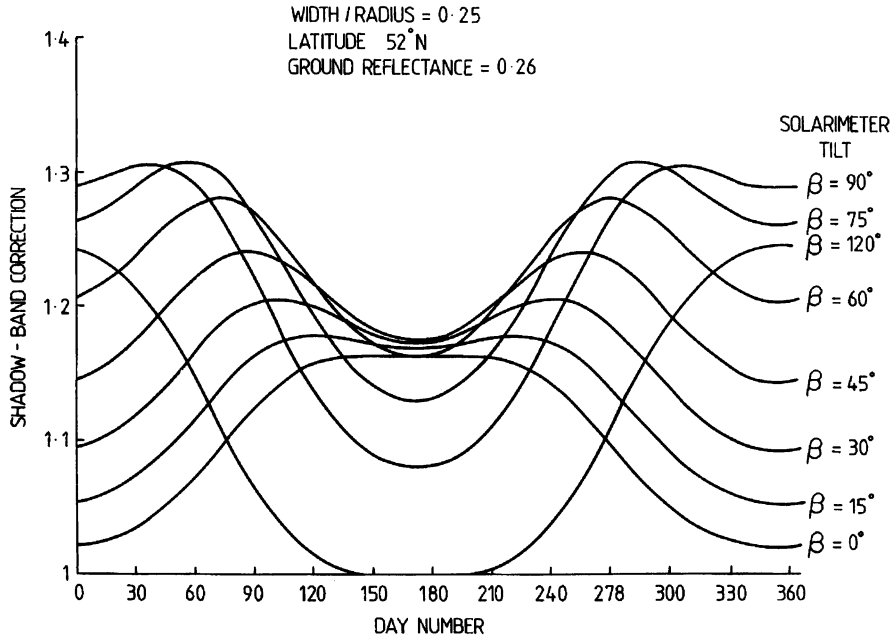


Fig. 2.9 Shadow-band correction factors for different pyranometer inclinations

correction for a pyranometer tilted to be perpendicular to the sun at solar noon. The correction factor increases as decreases with angle of tilt because although less radiation reflected from the ground is obscured by the shadow-band, the sky radiation which is obscured is a greater proportion of the total available. The variation of the shadow band correction factor throughout the year at different pyranometer inclination angles and a ground reflectance of 0.26 (appropriate for green grass) is shown in Fig. 2.9.

At low tilt-angles, the curve in Fig. 2.9 has a minimum in winter and twin maxima in summer. At high tilt-angles, this is reversed, with a single minimum in summer, due simply to such a small section of the shadow-band being operative, at high summer tilt-angles. Indeed, if it were tilted further, there would be no need for a shadow-band during those parts of the year because the sensing element would be shaded completely from direct insolation. In deriving Fig. 2.8 it has been assumed that no light is reflected from the inner surface of the shadow-band, though it has been suggested that a value of 0.1 may be appropriate for the reflectance of a matt black surface (LeBaron et al. 1980). For the shadow-band geometry and ground reflectance indicated in Fig. 2.8, the shadow-based correction factor varies from 1.02 to 1.29 during winter between the horizontal and vertical pyranometer orientations. The variation is greater for lower values of ground reflectance and for shadow-bands with large width-to-radius ratios. Thus the potential error from such factors is relatively small but is at least as large as that an anisotropic diffuse-radiation distribution may introduce (Spencer et al. 1982) to shadow-band corrections that assume the diffuse sky to be isotropic.

2.3 Prediction of Solar Energy

The amount and type of solar radiation data available determines if it is appropriate to;

- Estimate insolation from nearby meteorological records of sunshine duration and degree of cloud cover (Iqbal 1983; Reddy 1987)
- Estimate the diffuse component from measurements of global insolation only (Liu and Jordan 1960)
- The use of design data based on semi-empirical relations, e.g. Hottel's clear day (Hottel 1976) established for cloudless conditions, the grey day derived from averaging over cloudy conditions (Stine and Harrigan 1985), and Standard Atmospheres and or correlation with ambient temperature (Norton and Abu-Ebeid 1989)
- Use measurements of global and diffuse insolation on horizontal surfaces from the nearest insolation measuring weather station
- Use satellite data (Perez et al. 2002)

Empirical formulas can be used to estimate insolation for locations at which no measurements are available. In many meteorological stations Campbell-Stokes and similar recorders record direct insolation above 200 Wm^{-2} up to 1981 and 120 Wm^{-2} since 1981, (Iqbal 1983). This is the basis of the "hours of sunshine" often used in daily weather reports. The threshold level of direct insolation is somewhat analogous to the concept of solar radiation utilisability (see Sect. 2.5). The duration of sunshine hours can be converted to insolation via various forms of the Angstrom correlation using extraterrestrial insolation and the solar geometric day length (and, in some versions, other factors) as normalising parameters. The Angstrom correlation is given in Fig. 2.10 (Angstrom 1924; Prescott 1940; Page 1961). Given the now ready availability of measured insolation data, the practical use of the Angstrom-type correlations – even the most refined (Reddy 1987) – has become very limited.

Various climatological parameters such as humidity, temperature, rainfall, number of sunshine hours, total amount of cloud coverage, have been used in developing empirical relations as substitutes for the direct measurement of insolation. However, as attenuation of solar radiation travelling through the atmosphere is a complicated stochastic process, the utility of such approaches is limited.

2.3.1 *Insolation a Horizontal Plane*

The ratio of the diffuse component to total insolation is dependent on the monthly mean clearness index (Liu and Jordan 1960). The clearness index is the ratio of the monthly mean daily insolation on the earth's surface to the extraterrestrial irradiation, both measured on horizontal plane at the same latitude as shown in Fig. 2.11. Subsequent developments have provided correlations that account of seasonal

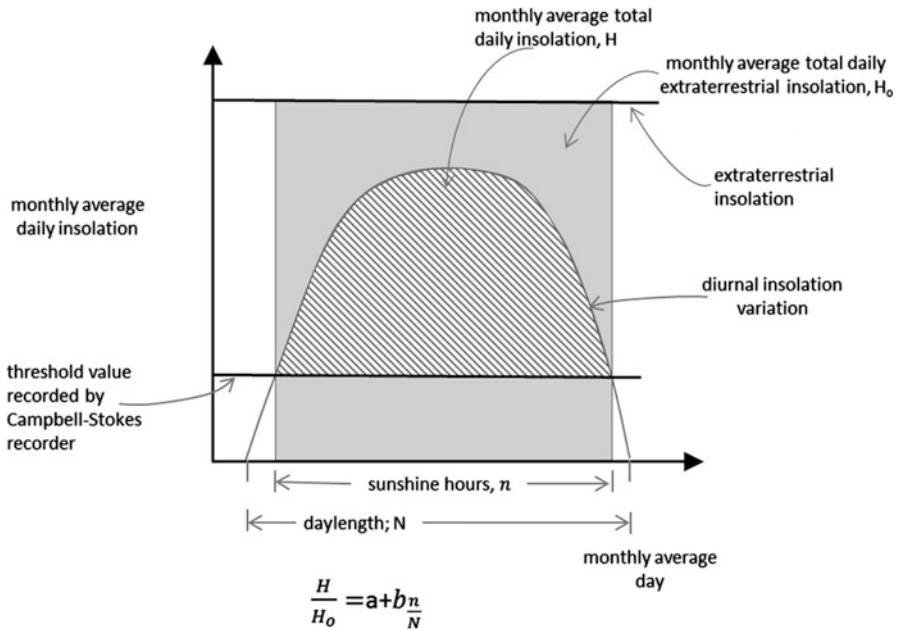


Fig. 2.10 Angstrom correlation of monthly-average daily insolation with apparent daylength

variations by including the sunset hour angle (Collares-Pereira and Rabl 1979; Erbs et al. 1982). It has been observed that for locations with similar climates there exist “generalised” cumulative frequency distribution curves for the daily clearness index as shown in Fig. 2.12 (Liu and Jordan 1963; Bendt et al. 1981; Theilacker and Klein 1980; Reddy et al. 1985; Hollands and Huget 1983). When the minimum and maximum average monthly clearness index are known, then the probability density function for clearness indices (Reddy 1987) can be produced as shown in Fig. 2.11.

Correlations that employ the clearness index are used to predict the daily diffuse component from the daily global incident insolation (Liu and Jordan 1960; Collares-Pereira and Rabl 1979) and can include seasonal variations as indicated by the sunset hour angle (Erbs et al. 1982) as shown in Fig. 2.13. Over the *long term*, in many climates, the diurnal variation of global insolation is symmetrical about solar noon (Liu and Jordan 1960). This observation has been used to develop a correlation between hourly and hourly and monthly mean daily horizontal global insulations (Collares-Pereira and Rabl 1979). Where the hour angle corresponds to the midpoint of the hour, expressions for hourly and monthly mean-daily horizontal diffuse components of insolation are shown in Fig. 2.13 (Liu and Jordan 1960). Hourly correlations of diffuse to global insolation have also been developed (Gordon and Hochman 1984; Erbs et al. 1982).

Monthly average clearness index K_T ; average atmospheric insolation attenuation at a specific location over a particular month.

$$K_T = \frac{I_G}{I_{B_o}}$$

I_{B_o} extraterrestrial irradiance varies with the eccentricity of the earth's orbit;

$$I_{B_o} = \frac{24}{\pi} S \left\{ 1 + 0.33 \cos \left(\frac{2\pi d_n}{365} \right) \right\} (\cos \phi \cos \delta \sin \omega_s + \omega_s \sin \phi \sin \delta)$$

S: Solar constant = 1367 W/m²

- d_n number of day in year
- ϕ latitude
- δ declination
- ω_s sunrise hour angle

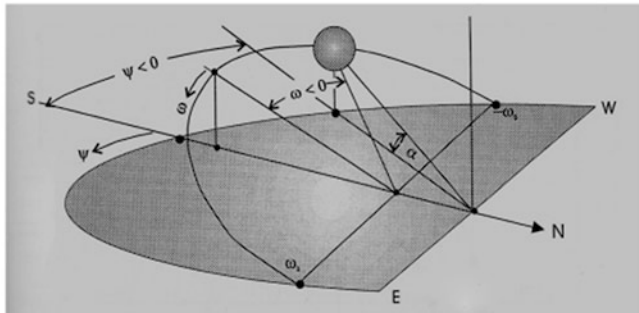
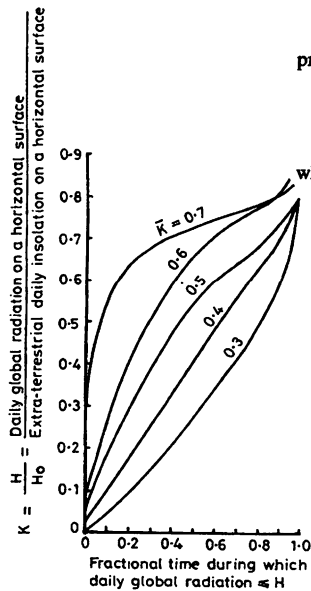


Fig. 2.11 Definition of clearness index



probability density function for clearness indices

$$P(K_T) = C \left[\frac{K_{T,max} - K_T}{K_{T,max}} \right]^n e^{\gamma K_T} \text{ for } K_{T,min} \leq K_T \leq K_{T,max}$$

where C is given by

$$C = \left[\int_{K_{T,min}}^{K_{T,max}} \left[\frac{K_{T,max} - K_T}{K_{T,max}} \right]^n e^{\gamma K_T} \right]^{-1}$$

cumulative frequency distribution is given by

$$F(K_T) = \int_{K_{T,min}}^{K_T} P(K_T) dK_T = \frac{\exp(\gamma K_{T,min}) - \exp(\gamma K_T)}{\exp(\gamma K_{T,min}) - \exp(\gamma K_{T,max})}$$

Fig. 2.12 Cumulative frequency distributions of daily clearness indices

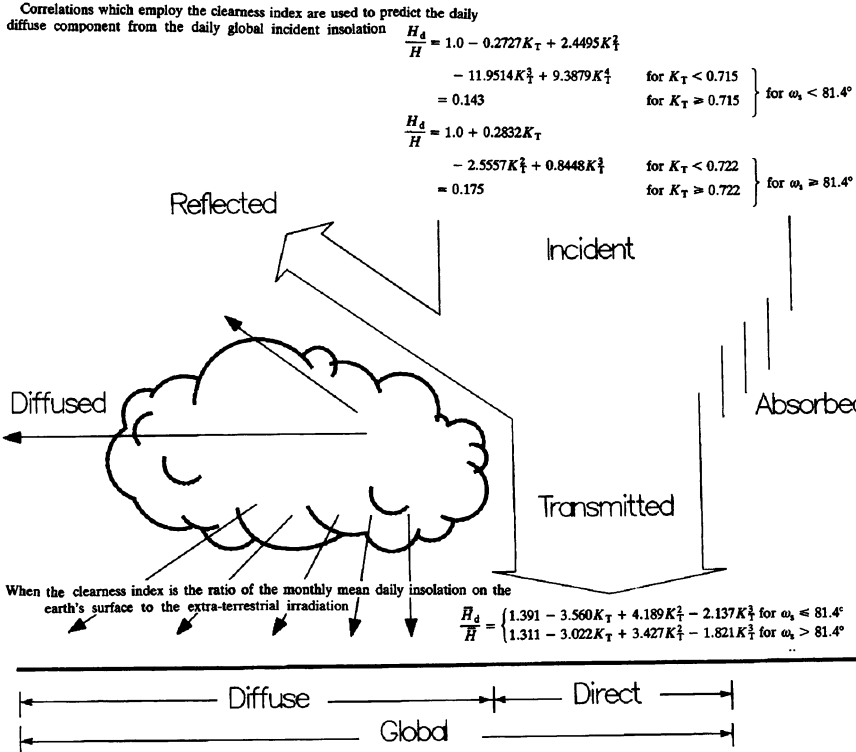


Fig. 2.13 Daily and monthly diffuse to total insolation correlations

2.3.2 Insolation on a Tilted Plane

Measured solar radiation data are now becoming available for an increasing range of locations in the form of hourly global and diffuse insolation on horizontal surfaces, and as monthly-averaged daily global insolation on horizontal surfaces. For a limited set of locations data is available for global insolation on tilted surfaces. However, it is not practicable to make measurements of global radiation on all the possible orientations of surfaces that may be needed, so calculations are used to derive radiation incident on such surfaces from horizontal surface measurements. Given a record of hourly solar radiation incident on horizontal surfaces it is possible to calculate the hourly incident energy on surfaces of any slope and orientation within the vicinity of the data-collection station. It is also possible to calculate the daily, monthly and annual incident energy for the year in question.

In calculating the insolation on an inclined plane most models treat the diffuse component like the beam component. This assumes that most of the diffuse

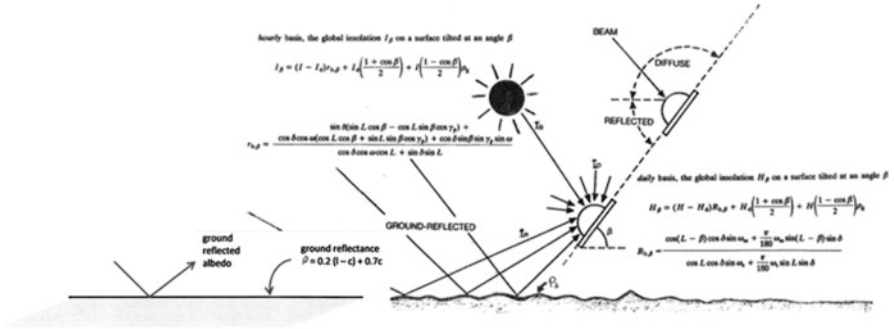


Fig. 2.14 Hourly and daily global insolation on a tilted plane

radiation comes from the circumsolar region of the sky, the implication being that most diffuse insolation arises from forward scattering. This approximation applies most closely to, and can be used for design purposes on cloudless days. The angular correction to be applied to the diffuse component is then the same as that for the beam component as shown in Fig. 2.14 which taken together with ignoring ground-reflected radiation, gives the total incident insolation on the inclined surface.

Figure 2.14 represents the “Liu and Jordan” (1962) model of insolation on inclined planes. This considers: beam radiation, diffuse solar radiation, and solar radiation diffusely reflected off the ground. It was assumed that, like isotropic diffuse solar radiation, ground-reflected radiation gives rise to an irradiance that is proportional to the appropriate view factor. A surface tilted at slope β from the horizontal has a view factor to the sky of $(1 + \cos(\beta))/2$, and that this is also the correction factor for an isotropic distribution of diffuse radiation. The view factor to the ground, assumed level and infinite in extent, must then be $(1 - \cos(\beta))/2$. If the ground is a perfectly diffuse reflector of constant diffuse reflectance (albedo) ρ for the global insolation, the radiation reflected off the ground onto the surface is shown in Fig. 2.14. The albedo ρ varies considerably between about 0.05 (for smooth water) and about 0.8 (for fresh snow), but most land surfaces have albedos around 0.2. A fractional time “C” (usually on a monthly basis) to represent duration of snow cover may be used, as shown in Fig. 2.14, to modify ground reflectance changes due to snow.

Liu and Jordan’s (1962) model assumes that the ground is a Lambertian reflector reflecting all wavelengths equally both uniformly in all directions, and independently of solar elevation. This assumption is usual in treatments of ground-reflected solar radiation (Dave 1977), but, in practice, albedos vary significantly with the wavelength and angle of incidence of the radiation, and with the angle of view of the observer.

On an hourly basis the global insolation on a tilted surface (Liu and Jordan 1960) is also shown in Fig. 2.14.

2.4 Use of Satellite Information to Produce Solar Energy Data

Geostationary satellites orbiting the earth measure ground and cloud reflected radiation. This information is collated and analysed to produce solar radiation maps for monthly and annual insolation averages to a spatial resolution of 10 km by 10 km. Hourly radiance images from satellites are combined with daily snow cover data together with monthly averages of atmospheric water vapour, absorbing gases and atmospheric aerosols to determine hourly direct and diffuse insolation on a horizontal surface (Marion and Wilcox 1994; Maxwell et al. 1998; George and Maxwell 1999; Perez et al. 2002).

2.5 Solar Radiation Utilisability

For many solar thermal systems there exists a critical, or threshold value of insolation. For solar collectors, this is that insolation for which at a given ambient temperature, the heat gained equals heat losses as illustrated on the left hand side of Fig. 2.15 for an ambient temperature that varies over a day. Assuming that the monthly mean ambient temperature lies midway between the corresponding ambient morning and evening temperatures give the insolation thresholds shown on the right-hand side of Fig. 2.15 for all days of a month a critical radiation ratio can be defined as shown in the right-hand side of Fig. 2.15.

When the ambient temperature remains constant, for a sinusoidal diurnal insolation pattern, the morning and evening thresholds of utilizable insolation are the same, a similar single value for the threshold of utilizable insolation can be calculated using a diurnal average ambient temperature. Solar radiation utilisability depends solely on insolation for a given location, month, the mean ambient temperature appropriate for the month and tilt of the system. The daily utilisability factor can be determined from the hourly utilisability fractions by weighting the

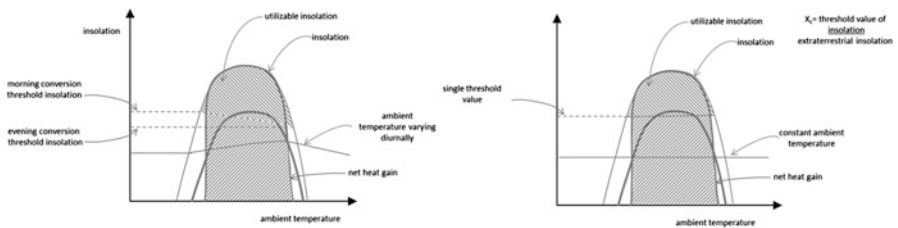


Fig. 2.15 Insolation utilisability threshold

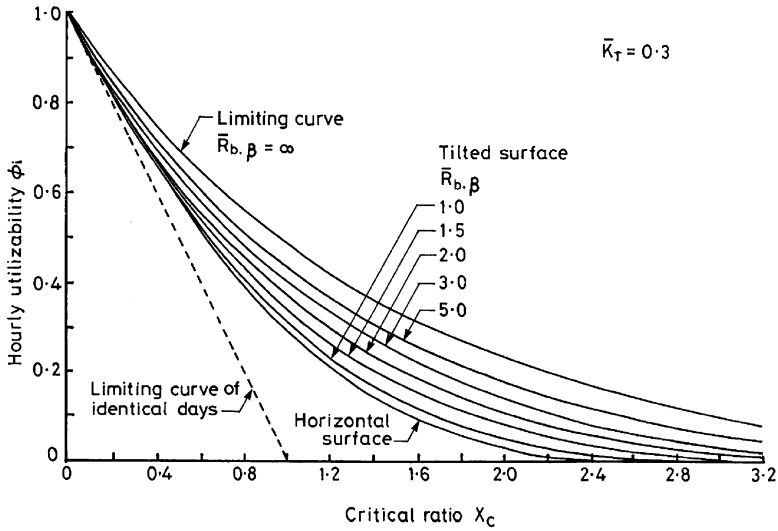


Fig. 2.16 Critical insolation ratio for different surface inclinations at a clearness index of 0.3

hourly insolation values (Clark et al. 1983). Generalizable hourly utilizability curves have been derived (Liu and Jordan 1965) from generalized clearness index curves. From those curves, the hourly utilizability on a monthly basis for equator-facing collectors can be deduced for different clearness indices, critical radiation ratios and different monthly average daily ratios of beam radiation on the tilted surface to that on a horizontal surface. These curves are illustrated in Figs. 2.16, 2.17 and 2.18. Similar forms of graph have been generated for generalised daily utilizability, (Klein 1978; Collares-Pereira and Rabl 1979; Theilacker and Klein 1980; Evans et al. 1982).

2.6 Daylight Data

Daylight is solar illumination in the interiors of buildings as perceived by the human eye. Solar radiation and the luminosity of daylight are related by the luminous efficacy of the radiation being considered. Luminous efficacy is defined as the quotient of luminous flux, as shown in Fig. 2.19. It is a function of the spectral distribution of the radiant energy and so varies with solar altitude, cloud cover, pollutant content of the atmosphere, and also the relative proportions of beam and diffuse radiation (Littlefair 1985, Robledo and Soler 2001).

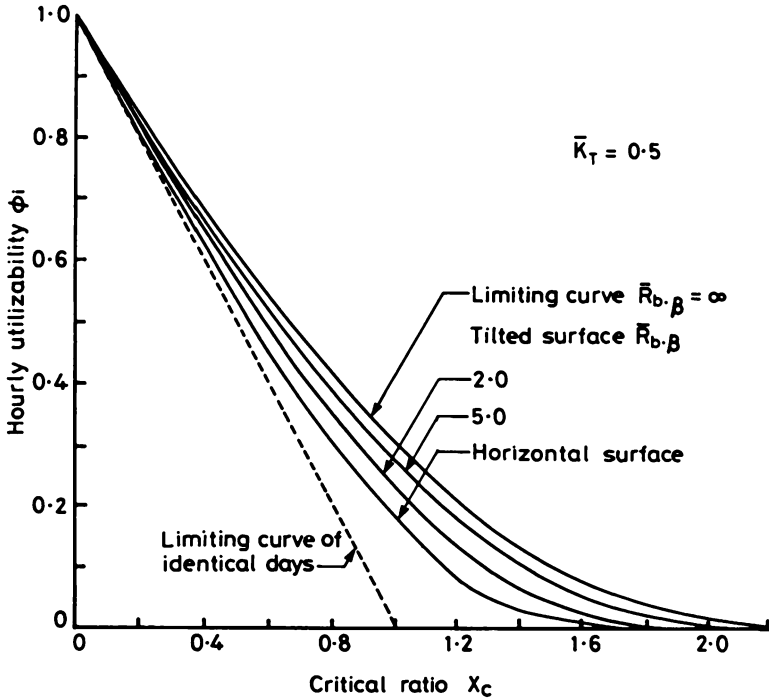


Fig. 2.17 Critical insolation ratio for different surface inclinations at a clearness index of 0.3

2.7 Geographical Availability of Solar Energy

A local climate is the consequence of a distinctive regional combination and interrelation of insolation, temperature, precipitation, humidity and wind speed and direction as driven by global air and ocean circulations, latitude above sea level and topography. The world can be divided into several distinctive climatic types (Trewartha and Horn 1980) as shown in Fig. 2.20 and Table 2.1. The global distribution of insolation is shown in Fig. 2.21. Although latitudinal, variations of insolation may be seen for high latitudes, there are also appreciable longitudinal variations (particularly at equatorial latitudes) due to the alternation of continents and oceans over the earth’s surface.

In addition to these macroscale factors, which determine climate type, mountainous and urban regions also have mesoclimatic effects. Urban areas often receive less insolation than their rural surroundings: the sunshine duration in industrial areas can be reduced by up to 20 % (Landsberg 1981). This reduction is largest at low solar elevations when the air mass is longest. Different impacts can arise seasonally in temperate climates, for example, if frequent low-level atmospheric inversions occur in winter and autumn, they contribute to the accumulation of pollutants and hence to solar radiation attenuation and a concomitant increased

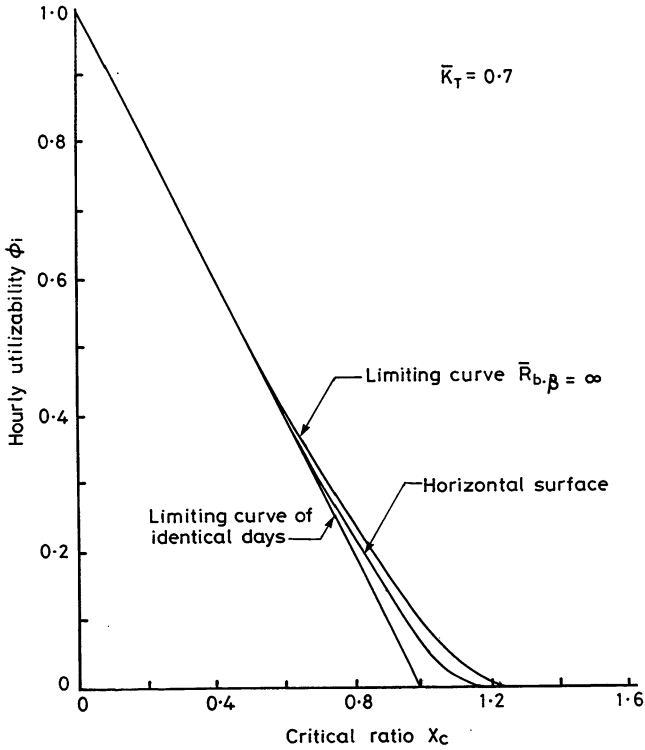


Fig. 2.18 Critical insolation ratio for a typical “clear” sky with a clearness index of 0.7 showing the limited change in solar energy utilizability in sunny climates

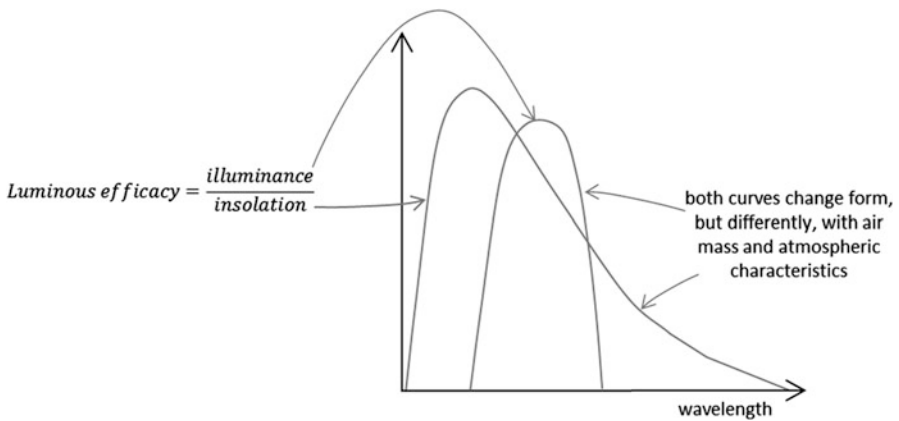


Fig. 2.19 Definition of luminous efficacy

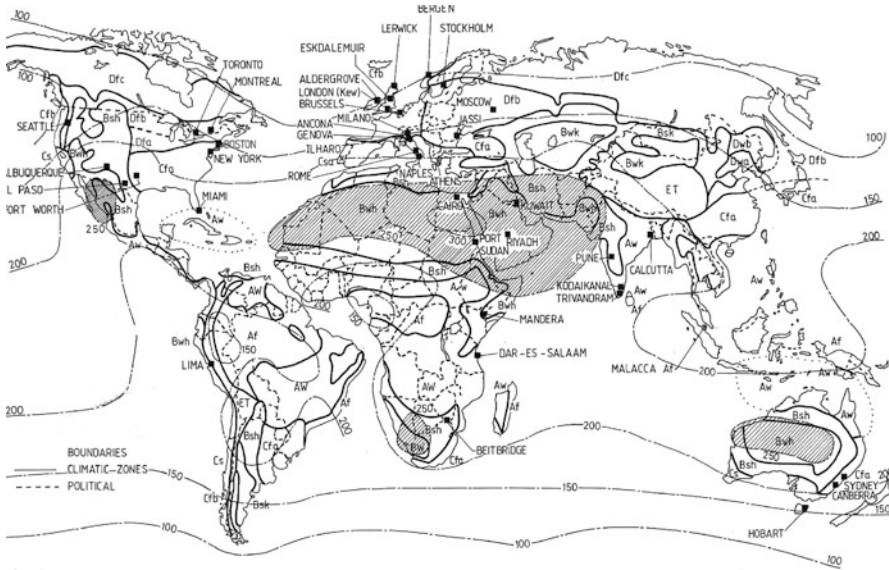


Fig. 2.20 Distribution of world climate types

Table 2.1 Climate types

Designation	Description
Aw	Tropical wet and dry climate: high temperature throughout the year, dry season in low insolation period or winter. At least 1 month had less than 6 cm of rain
Bsh	Semi-arid climate or steppe: average annual temperature over 18 °C. These locations are low-latitude, or tropical
Bwh	Arid climate or desert, average annual temperature over 18 °C
Cfa	No distinct dry season; the driest month of summer receives more than 3 cm of rain, hot summer average temperature of warmest month over 22 °C
Cfb	No distinct dry season; the driest month of summer receives more than 3 cm of rain, cool summer average temperature of warmest month under 22 °C
Csa	Summer dry: at least three times as much rainfall in the wettest month of winter as in the driest month of summer. Hot summer average temperature of warmest month over 22 °C
Dfb	Cold climate: humid winters and cool summer, average temperature of warmest month under 22 °C
Af	Tropical wet climate, rainfall of the driest month is at least 6 cm. Within this climate there is a minimum of seasonal variation in temperature and precipitation, both remaining high throughout the year
Bwk	Arid climate or desert, average temperature under 187 °C. These locations are middle-latitude, or cold desert and steppes
Csb	Summer dry, at least three times as much rain in the wettest month of winter as in the driest month of summer, and the driest month of summer receives less than 3 cm
Dfa	Cold climate with humid winters, hot summer, average temperature of warmest month over 22 °C
Dfc	Cold climate with humid winters, cool short summer, less than 4 months over 10 °C
ET	Tundra climate, average temperature of warmest month below 10 °C but above 0 °C

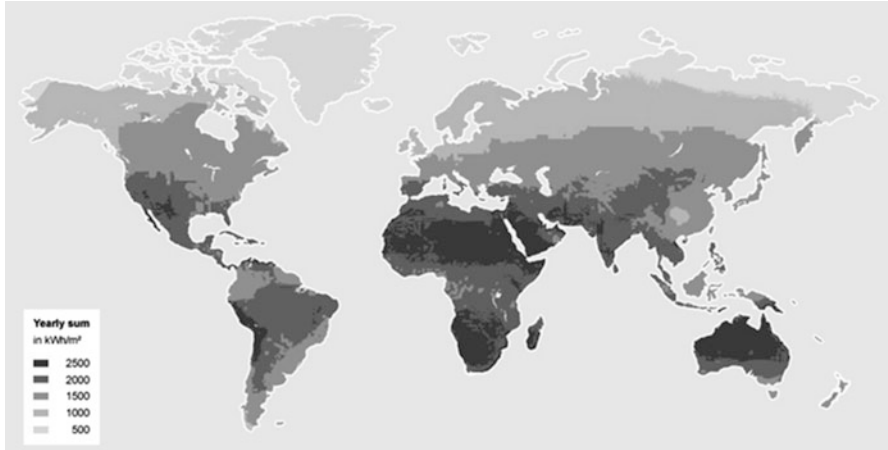


Fig. 2.21 Global distribution of insolation

diffuse component. However, again in temperate climates, in spring, generally-higher wind velocities and, in summer, greater atmospheric convection, both disperse pollutants with a relatively-smaller ensuent reduction in insolation. Maximum and minimum monthly values for ambient air temperatures lag very approximately a month behind those of the solar radiation: a manifestation of conduction of heat into, or out of, the ground. This lag is greater over the oceans at middle latitudes. The lag between temperature and insolation has been employed to develop an means of estimating monthly insolation from temperature data (Norton and Abu-Ebeid 1989).

For medium temperature applications, the ambient temperature can be a significant determinant of collector heat losses. The combination of different variations in cloud cover and ambient temperature can lead to solar thermal systems in ostensibly similar locations exhibiting very different behaviour. As an illustration of this, Fig. 2.22 shows that the numbers of days that a specified hot water demand can be met by an specific solar water heater across Europe. Insolation in winter determines the collector employed when very high solar savings fractions are sought. As can be seen from Fig. 2.22 in Europe, in locations such as Cyprus, solar water heater appropriately designed should be able to satisfy hot water demand all year round. In northern Europe as the same solar water heater is obviously unable to do this; as shown in Fig. 2.23, even if collector area is doubled from 5 to 10 m² in a northern European climate only a relatively small space heating solar fraction is achieved. The design of solar thermal system has to include interseasonal heat storage if a high solar function is required as shown in Fig. 2.24.

Though an interseasonal heat storage system may give a larger solar function, for water heating in particular this may be only in terms of energy not exergy, that is the desired end-use temperature may not be satisfied in winter and auxiliary energy will be used.

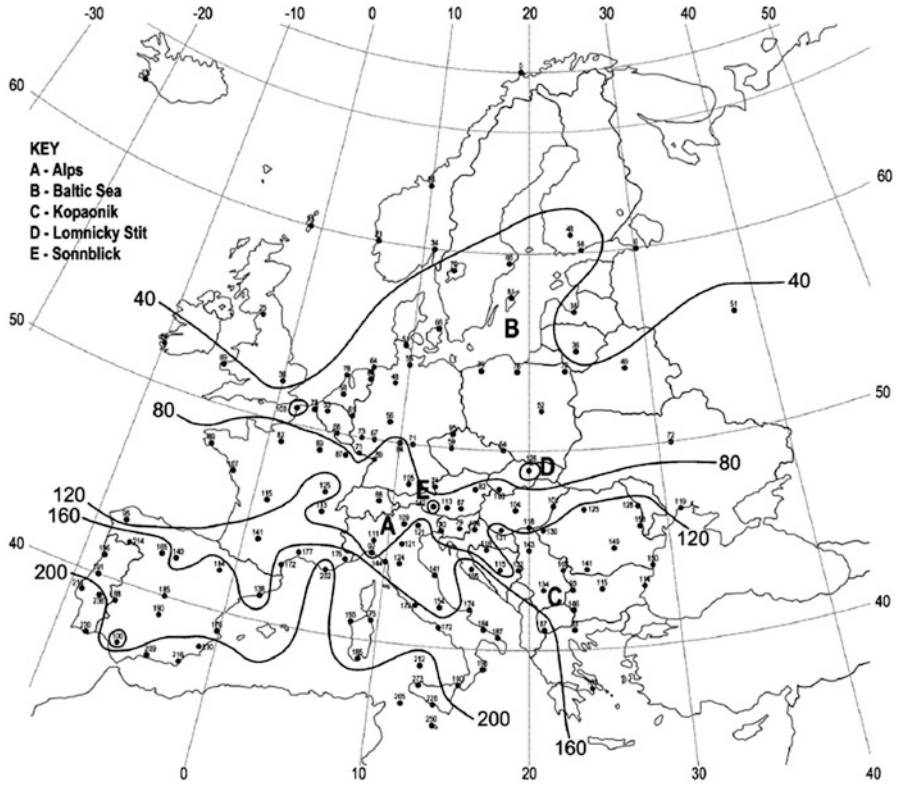


Fig. 2.22 Map of number of days of solely-solar hot water provision

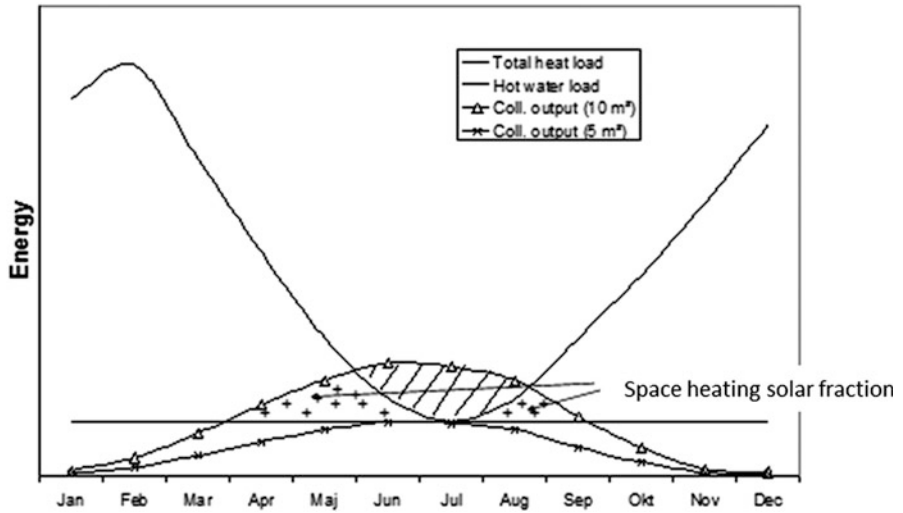


Fig. 2.23 Annual output for two specific collector areas

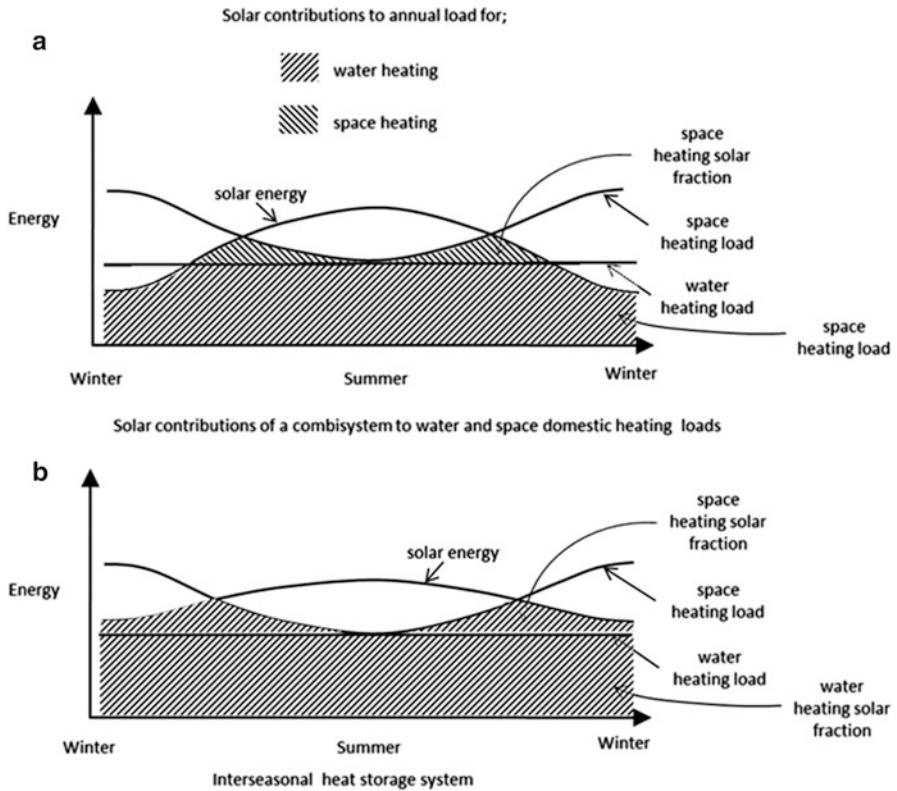


Fig. 2.24 Illustrative annual variations of average diurnal solar contributions of different solar energy systems for water and space heating loads in temperate climates

The geographic variation in the diurnal and annual variation of diffuse insolation is a critical factor limiting the use of concentrating collectors that collect solely direct insolation. The annual direct component at normal incidence is employed as a key selection factor for determining the most appropriate locations worldwide, as shown in Fig. 2.25, for concentrating solar thermal power generation. The example of Ghana, enlarged in Fig. 2.25, illustrates that there are very significant local variation in annual direct normal solar radiation, particularly in equatorial regions with monsoon or rainy seasons.

2.8 Solar Geometry

Solar energy originates in the interior regions of the Sun as a result of a hydrogen fusion reaction. Normal to the Sun’s rays at the average sun-earth distance of 1.5×10^{11} m, the intensity of solar radiation incident per unit area measured

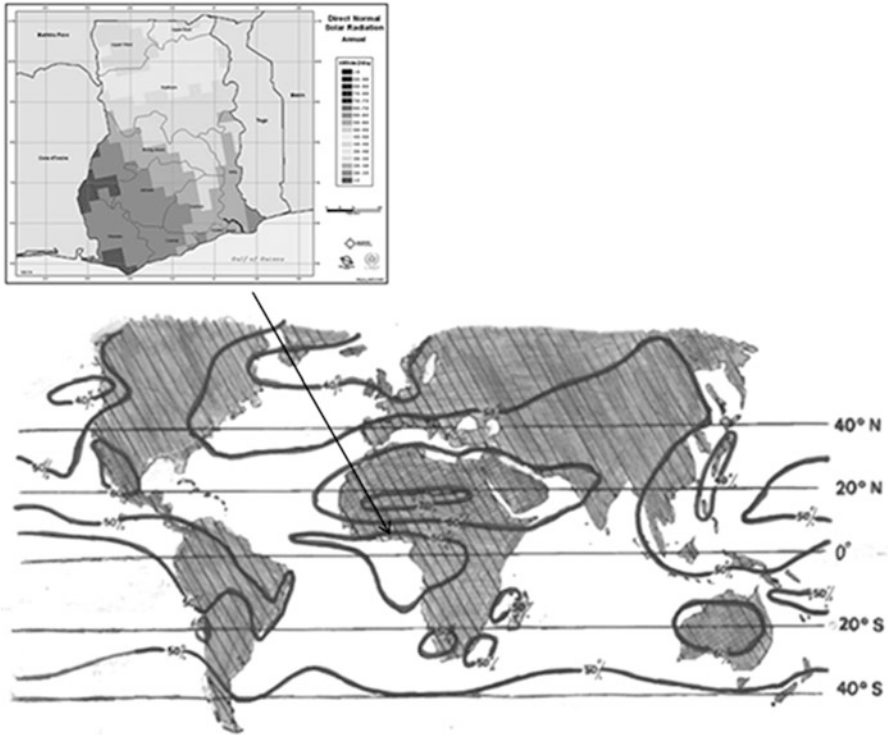


Fig. 2.25 Map indicating regions suitable for concentrating solar thermal power generation

outside the earth’s atmosphere, is $1,367 \text{ W/m}^2$, this is called the solar constant. As the Earth’s orbit is slightly elliptical, the intensity of radiation received outside the Earth’s atmosphere varies $\pm 3.4 \%$ over the year with the maximum intensity at the perihelion and the minimum at aphelion (Stine and Harrigan 1985).

Solar radiation varies over each day due to,
Geometrical factors:

- Influence of the slope and orientation of a surface on its interception of insolation;
- Obstruction of beam and diffuse solar radiation by neighbouring structures;
- Reflection of solar radiation from adjacent surfaces.

Physical factors:

- Total intensity and beam and diffuse insolation proportions due to changes in atmosphere conditions,
- The distribution of diffuse radiation over the sky and
- The variation of ground reflectance due to changes in ground conditions due to vegetation or snow.

2.9 Skyward Distribution of Diffuse Insolation

Air molecules (i.e. nitrogen, oxygen and other constituents) scatter radiation in very short wavelengths comparable to the size of molecules; this is called the Rayleigh scattering. Water droplets and aerosols scatter radiation whose wavelengths are comparable to the diameters of such particles. Therefore, an increase in the turbidity or dust content of the atmosphere or the cloud cover increases the scattering of solar radiation. As a result of scattering, part of the direct radiation is converted into diffuse radiation. Higher turbidity and cloud coverage increase the scattering of longer wavelength radiation which in turn causes the sky to be increasingly white. As a result of atmospheric scattering, some incident solar radiation is reflected back into outer space, while some of the scattered radiation reaches the earth's surface from all directions over the sky as diffuse radiation. Solar radiation that is neither scattered nor absorbed by the atmosphere, reaches the earth's surface as direct radiation. These processes are illustrated schematically in Figs. 2.12 and 2.13.

Diffuse solar radiation is usually anisotropic due to

- Overcast cloud
- Circumsolar brightening
- Horizon brightening and
- Broken cloud.

Broken cloud is a major cause of diffuse radiance anisotropy. An overcast sky of uniform cloud thickness, however, will be brighter near the zenith than near the horizon. This is opposite to the horizon brightening that occurs for a clear sky. Circumsolar brightening is caused by the strong tendency of dust matter suspended in the atmosphere, to scatter light by Mie scattering in the forward direction. Gas molecules scatter light by Rayleigh scattering which occurs equally in all directions. Thus, most of the beam radiation that is scattered by dust will deviate in a cone from the solar direction by only a few degrees from the direct beam. Consequently an isotropic sky around the Sun can have an insolation intensity up to ten times the mean skyward insolation depending on atmospheric dust content. Where air is very clear the circumsolar diffuse radiation is small, whereas in highly dusty or polluted air it produces a totally overcast sky. Atmospheric Rayleigh and Mie scattering give rise to spatially homogeneous turbidity that can be amenable to physical modelling (Kittler 1986). Clouds introduce spatial heterogeneity across a sky that can alter rapidly. Intermittent partial cloud cover is not modelled readily to produce generalizable predictions that can be compared with measurements. Indeed, conversely, it is correlation parameters obtained from measurements that enable the effects of partial cloud cover to be included in insolation models; for example the Perez tilted irradiance model (Perez et al. 1983, 1990a, b, c, 1993), includes two such parameters – a sky clearness parameter based on the ratio between the direct normal radiation and the diffuse horizontal radiation and a sky brightness parameter defined as the ratio of diffuse to extraterrestrial insolation. The sky brightness parameter is necessary to describe cloud opacity as the sky clearness parameter is constant under cloudy skies.

Even under cloudless skies the sky clearness parameter can inadequately represent turbid conditions.

Horizon brightening of clear skies arises because of greater the air mass traversed by insolation near the horizon which causes more insolation to be scattered toward the observer from near the horizon than from higher parts of the sky. This effect is due principally to Rayleigh scattering but will be enhanced by the presence of atmospheric dust that will be concentrated largely at low altitudes giving rise to low elevation Mie scattering.

To estimate the error introduced when assuming isotropic diffuse solar radiation, the diffuse radiance distribution was calculated from first principles for an atmosphere with no absorption or non-homogeneity (Dave 1977). It was found that the assumption of isotropy would underestimate the diffuse insolation by a factor between 1 and 6. Liu and Jordan's (1962) model agrees well with observation at low irradiances ($<300 \text{ Wm}^{-2}$), i.e. when the sky is overcast and the isotropic assumption is most valid but at higher irradiances $>500 \text{ Wm}^{-2}$, Liu and Jordan's model underestimated the irradiance on tilted surfaces by 3–20 % (Klucher 1979). Liu and Jordan's model is also deficient in predicting insolation on tilted surfaces for non-uniform clear but partly cloudy sky conditions (Klucher 1979).

Circumsolar diffuse insolation, when present in will cause measured diffuse insolation on an equator-facing surface to be greater than the diffuse insolation predicted from models that assume an isotropic sky (Lloyd 1984). Conversely, on a polar-facing surface when predicted assuming isotropy diffuse insolation will be overestimated. Horizon brightening renders insolation measured in any inclined plane greater than that predicted when assuming an isotropic sky. Predictions of global irradiance, assuming an isotropic diffuse insolation distribution, will be about 5 % too low for equator-facing surfaces and about 40 % too high for polar-facing surfaces (Lloyd 1984) but as insolation on a pole-facing surface is smaller (except for early and late parts of the day in summer at high latitudes), the absolute difference between measured and predoctral diffuse insolation will be similar for both these orientations.

The diffuse insolation distribution provided by Klucher's anisotropic 'all-sky' model (Klucher 1979) agreed with observation to within 5 % on average. It is based on the earlier 'clear-sky' model of Temps and Coulson (1977) who in turn applied two correction factors to the diffuse solar radiation term Liu and Jordan's approach. These factors were intended to represent the regions of anisotropy found in another more uniform overcast the diffuse radiance distribution Klucher (1979) extended Temps and Coulson's model by including a modulating function so that it could be used in all sky conditions, from clear to overcast.

Under overcast conditions, when the ratio of diffuse to global insolation, is unity, the all-sky anisotropic model reduces to the Liu and Jordan isotropic model. For a clear sky, when the ratio of diffuse to global is small, the all-sky model approximates to the Temps and Coulson clear-sky model. Like Liu and Jordan, Hay (1979) resolved the total insolation on a tilted surface into three components: beam, diffuse and ground-reflected. Hay's anisotropic model differs from that of Liu and Jordan by assuming that all anisotropy in the diffuse insolation distribution on the tilted

surface a circumsolar term is associated with circumsolar brightening as shown in Fig. 3.19. The two components are expressed in terms of a clearness index.

A comparison of models of diffuse solar radiation against three month's insolation data (Hogan and Loxsom 1981) concluded that neither Liu and Jordan's (1962) isotropic model, Hay's anisotropic model (Hay 1979) nor Klucher's all-sky model (Klucher 1979) provided accurate predictions for vertical surfaces. Klucher's all-sky model produced the most consistently correct results for their limited data base. Comparing the ground-reflection term used, Hogan and Loxom (1981) found that Klucher's model performed better than the other two, either with or without it. For example, the Klucher model correctly predicted the measured hourly global insolation 98.5 % of the time for a south-facing surface tilted at 20°. However, the same model showed significant errors in the predictions for vertical surfaces, facing either north, south, east or west, more than 50 % of the time. These three models were compared again (Ma and Iqbal 1983) using data collected at Woodbridge, Ontario. It was shown that Hay's and Klucher's models were equally accurate, and superior to Liu and Jordan's model, in predicting the insolation on inclined south-facing surfaces. The isotropic model underestimated the insolation consistently throughout the year; Hay's model also underestimated constantly but by a smaller amount; Klucher's model overestimated in summer and underestimated in winter. The maximum root mean square error for Klucher's and Hay's model was less than 15 % for slopes of up to 60°. All three models produced large errors at steep slopes (Ma and Iqbal 1983).

A model that compares favourably with those of Liu and Jordan and Hay and Klucher has been developed that includes (Perez et al. 1986):

- A geometrical representation of the sky dome incorporating independently variable circumsolar and horizon brightening;
- A parametric description of the insolation conditions,
- An experimentally-derived variation of circumsolar and horizon brightening with the insolation conditions.

Obstruction on the amount of solar radiation reaching a surface can cause

- The complete attenuation of beam radiation to form a shadow.
- Reduction of the diffuse component of the global insolation received.
- Less ground-reflected component to be incident
- Enhanced diffuse and specular reflection of insolation from its surfaces

The magnitude of these components will depend on the secularity and reflectance of the obstruction and incident angles and intensity of the insolation on its surfaces. Evaluating the solar energy lost and/or reflected to a surface by overshadowing requires numerical integration. Much work has been done on the analysis of shading geometries amenable to exact calculation as where analytical solutions can be found, they yield quicker results than those found by numerical integration (Sharp 1981, 1982).

References

- Angstrom A (1924) Solar and terrestrial radiation. *Q J Roy Meteorol Soc* 150:121–126
- Bendt P, Collares-Pereira M, Rabl A (1981) The frequency distribution of daily insolation values. *Solar Energy* 27:1–5
- Burek SAM, Norton B, Probert SD (1988) Analytical and experimental methods for shadow-band correction factors for solarimeters on inclined planes under isotropically-diffuse and overcast skies. *Solar Energy* 40(2):151–160
- Clark DR, Klein SA, Beckman WA (1983) Algorithm for evaluating the hourly radiation utilizability function ASME. *J Solar Energy Eng* 105:281–287
- Collares-Pereira M, Rabl A (1979) Simple procedure for predicting long term average performance of non-concentrating and of concentrating solar collectors. *Solar Energy* 23:235–253
- Dave JV (1977) Validity of the isotropic-distribution approximation in solar energy estimations. *Solar Energy* 19:331–333
- Drummond AJ (1956) On the measurement of sky radiation. *Arch Met Geophys Bioklim* B7:413–436
- Erbs DG, Klein SA, Duffie JA (1982) Estimation of the diffuse radiation fraction for hourly, daily and monthly – average global radiation. *Solar Energy* 28:293–302
- Evans DL, Rule TT, Wood BD (1982) A new look at long term collector performance and utilizability. *Solar Energy* 28:13–23
- George R, Maxwell E (1999) High-resolution ways of solar collector performance using a climatological solar radiation model. In: *Proceedings of the annual conference of the American Solar Energy Society, Portland*
- Gordon JM, Hochman M (1984) On correlations between beam and global radiation. *Solar Energy* 32:329–336
- Hay JE (1979) Study of shortwave radiation on non-horizontal surfaces. Canadian Climate Center. Report 79–12, AES, Downview
- Hogan WD, Loxsom FM (1981) Preliminary validation of models predicting insolation on tilted surfaces. In: *Proceedings of the annual meeting of the American section of the international solar energy society*
- Hollands KGT, Huget RG (1983) A probability density function for the clearness index, with applications. *Solar Energy* 30:195–209
- Hottel HC (1976) A simple model for estimating the transmittance of direct solar radiation through clear solar atmospheres. *Solar Energy* 18
- Ineichen P, Gremaud JM, Guisan O, Mermoud A (1983) Study of the corrective factor involved when measuring the diffuse solar radiation by use of the ring method. *Solar Energy* 31:113–117
- Iqbal M (1983) *An Introduction to solar radiation*. Academic, Toronto
- Kittler R (1986) Luminance model of homogeneous skies for design and energy performance predictions. In: *Proceeding of the 2nd international daylighting conference, Long Beach*
- Klein SA (1978) Calculation of flat-plate collector utilizability. *Solar Energy* 21:393–402
- Klucher TM (1979) Evaluation of models to predict insolation on tilted surfaces. *Solar Energy* 111–114
- Landsberg HE (1981) *The urban climate*. Academic, New York
- LeBaron BA, Peterson WA, Dirmhirn I (1980) Corrections for diffuse irradiance with shadowbands. *Solar Energy* 25:1–13
- Littlefair PJ (1985) The luminous efficacy of daylight, a review. *Light Res Technol* 17:162–182
- Liu BYH, Jordan RC (1960) The interrelationship and characteristic distribution of direct, diffuse and total solar radiation. *Solar Energy* 4:1–19
- Liu BYH, Jordan RC (1962) Daily insolation on surfaces tilted towards the equator. *Trans ASHRAE* 526–541
- Liu BYH, Jordan RC (1963) A rational procedure for predicting the long-term average performance of flat-plate solar energy collectors. *Solar Energy* 7:53–74

- Liu BYH, Jordan RE (1965) Performance and evaluation of concentrating collectors for power generation trans. ASME Journal of Engineering for Power 87:1–7
- Lloyd PB (1984) Solar energy for engineers. Helios 22: Solar energy unit, University College, Cardiff
- Lunde PJ (1980) Solar thermal engineering. Wiley, New York
- Ma CCY, Iqbal M (1983) Statistical comparison of models for estimating solar radiation on inclined surfaces. Solar Energy 31:31–317
- Marion W, Wilcox S (1994) Solar radiation data manual for flat plate and concentrating collectors. Report NREL/TP-463-5607, National Renewable Energy Laboratory, Golden
- Maxwell E, George R, Wilcox S (1998) A climatological solar radiation model. In: Proceedings of the annual conference of the American solar energy society, Albuquerque
- Mujahid A, Turner WD (1980) Diffuse sky measurements and determination of corrected shadow band multiplication factors. ASME annual winter meeting, paper no 80-WA/Sol-26
- Norton B, Abu-Ebeid M (1989) Estimation of mean monthly daily total insolation from mean monthly daily ambient temperature. Ambient Energy 10:151–162
- Page JK (1961) The estimation of monthly mean values for daily total short wave radiation on vertical and inclined surfaces from sunshine hours for latitudes 40°N to 40°S. In: Proceedings of the UN conference on new sources of energy, Rome, pp 378–390
- Painter HE (1981) The shade ring correction factor for diffuse irradiance measurements. Solar Energy 26:361–363
- Perez R, Scott JT, Stewart R (1983) An anisotropic model for diffuse radiation incident of hopes of different orientations and possible applications to CPCs. Prog Solar Energy 6:883–888
- Perez R, Stewart R, Arbogast C, Seals R, Scott J (1986) An anisotropic hourly diffuse radiation model for sloping surfaces: description, performance validation, site dependency evaluation. Solar Energy 36:481–497
- Perez R, Ineichen P, Seals R, Zelenka A (1990a) Making full use of the clearness index for parameterising hourly insolation conditions. Solar Energy 45:111–114
- Perez R, Ineichen P, Seals R, Michalsky J, Stewart R (1990b) Modeling daylight availability and irradiance components from direct and global irradiance. Solar Energy 44:271–289
- Perez R, Seals R, Zelenka A, Ineichen P (1990c) Climatic evaluation of models that predict hourly direct irradiance from hourly global irradiance; prospects for performance improvements. Solar Energy 44:99–108
- Perez R, Seals R, Michealsky J (1993) An all-weather model for sky luminance distribution – a preliminary configuration and validation. Solar Energy 50:235–245
- Perez R, Ineichen P, Moore K, Kmiecik M, Chain C, George R, Vignola F (2002) A new operational satellite-to-irradiance model. Solar Energy 75:307–317
- Prescott JA (1940) Evaporation from water surface in relation to solar radiation. Trans Roy Soc 54:114–118
- Rawlins F, Readings CJ (1986) The shade ring correction for measurements of diffuse irradiance under clear skies. Solar Energy 37:407–416
- Reddy TA, Kumar S, Saunier GY (1985) Review of solar radiation analysis techniques for predicting long-term thermal collector performance – applicability to Bangkok data. Renew Energy Review J 7:56–80
- Reddy SJ (1987) The estimation of global solar radiation and evaporation through precipitation. Solar Energy 38:97–104
- Robinson N, Stoch L (1964) Sky radiation measurements and correction. J Appl Meteorol 3:179–181
- Robledo L, Soler A (2001) On the luminous efficiency of diffuse solar radiation. Energy Convers Manage 42:1181–1190
- Sharp K (1981) Sun angles and shading analysis for surfaces at any tilt or azimuth. In: Proceedings of the 1981 annual meeting, AS/ISES
- Sharp K (1982) Calculation of monthly average insolation on a shaded surface at any tilt and azimuth. Solar Energy 28:531–538

- Spencer DW, Oettinger BS, Stewart R (1982) Diffuse band correction factors for short time intervals. Progress in solar energy. In: Proceedings annual general meeting of the American Solar Energy Society, pp 1253–1257
- Steven MD, Unsworth MH (1980) Shade-ring corrections for pyranometer measurements of diffuse solar radiation from cloudless skies. *Quart J Royal Meteorol Soc* 106:865–872
- Stine WB, Harrigan RW (1985) Solar energy fundamentals and design. Wiley, New York
- Temps RC, Coulson KL (1977) Solar radiation incident upon slopes of different orientations. *Solar Energy* 19:179–184
- Theilacker JC, Klein SA (1980) Improvements in the utilizability relationships. American Section of the international solar energy society. Proceedings, Phoenix, pp 271–275
- Trewartha GT, Horn LH (1980) An introduction to climate, 5th edn. McGraw-Hill, New York
- Van den Brink GJ (1982) Climatology of solar irradiance on inclined surfaces IV- part II. Validation of calculation models, Royal Dutch Meteorological Institute (KNMI). Final report: EEC contract no ESF-006-80 NL (B)



<http://www.springer.com/978-94-007-7275-5>

Harnessing Solar Heat

Norton, B.

2014, XVII, 258 p. 193 illus., 7 illus. in color.,

ISBN: 978-94-007-7275-5